

Changes in the gradient percolation transition caused by an Allee effect

Michael T. Gastner,^{1,2} Beata Oborny,³ Alexey B. Ryabov,¹ and Bernd Blasius¹

¹*Institute for the Chemistry and Biology of the Marine Environment, Carl von Ossietzky Universität, Carl-von-Ossietzky-Straße 9-11, 26111 Oldenburg, Germany*

²*Department of Mathematics, Complexity and Networks Programme,*

Imperial College London, South Kensington Campus, London SW7 2AZ, United Kingdom

³*Department of Plant Taxonomy and Ecology, Loránd Eötvös University, Pázmány Péter stny. 1/C, H-1117, Budapest, Hungary*

The establishment and spreading of biological populations depends crucially on population growth at low densities. The Allee effect is a problem in those populations where the per-capita growth rate at low densities is reduced. We examine stochastic spatial models in which the reproduction rate changes across a gradient g so that the population undergoes a 2D-percolation transition. Without the Allee effect, the transition is continuous and the width w of the hull scales as in conventional (i.e., uncorrelated) gradient percolation, $w \propto g^{-0.57}$. However, with a strong Allee effect the transition is first order and $w \propto g^{-0.26}$.

PACS numbers: 87.23.Cc, 87.10.Hk, 87.10.Mn, 05.40.-a

It is not just human relationships which obey the rule “two’s company, three’s a crowd.” Negative density dependence, defined as a decrease of the per-capita growth rate with increasing population density, is common among almost all species at high densities, where overcrowding and the depletion of resources limit further growth. The most common model for negative density dependence is the logistic equation which assumes that the per-capita growth rate decreases linearly with the population size P ,

$$\frac{1}{P} \frac{dP}{dt} = r \left(1 - \frac{P}{K} \right), \quad (1)$$

where t is time, r is the intrinsic rate of increase, and K the carrying capacity.

If $r, K > 0$, Eq. 1 is characterized by a negative density dependence for all population sizes P . For some small populations, however, a positive density dependence can be observed. The latter is called a demographic Allee effect, named after Warder Clyde Allee, who described it first and supported the theory with examples from various animal species from insects to mammals [1]. Small populations can suffer from reduced growth rates for various reasons. Frequently, a collective behavior (e.g., defense against predators) becomes inefficient when the group is small. Additionally, small populations are less efficient in modifying the environment to their own benefit. For example, plant individuals in aggregations can reduce frost or desiccation, but only when the density in the clump is sufficiently high [2]. To generalize density dependence, Volterra proposed to replace the right-hand side of Eq. 1 with a quadratic function of P [3],

$$\frac{1}{P} \frac{dP}{dt} = -A + BP - CP^2, \quad A, B, C > 0. \quad (2)$$

If $B^2 - 4AC > 0$, Eq. 2 has two stable fixed points, unlike Eq. 1, which has only one, so that the long-term behavior of Eq. 2 depends on the initial population density. If

$P > (B - \sqrt{B^2 - 4AC})/2C$ at $t = 0$, the population will approach a positive limit, whereas a smaller initial population will become extinct. Several other formulations of the Allee effect have been suggested in the past decades, some including stochastic and spatial effects [4, 5] (see chapter 3.5 in Ref. 6 for a review). They all have in common that a strongly positive density dependence accelerates the extinction of small populations.

The work described here is motivated by the question: what are the consequences of an Allee effect on populations that live at a margin of a geographic range? Because such populations usually have low densities, one can expect that it matters greatly for the success of establishment and spreading if an Allee effect is present or not [5, 7]. In this Letter, we investigate the situation near a geographic margin with two models where the density changes across space from low to high values. We show that a strong Allee effect makes the percolation transition at the margin discontinuous, causing scaling behavior different from previously studied types of gradient percolation [8, 9].

Our models are stochastic cellular automata whose local rules correspond to discretized versions of Eq. 1 or 2. Both cellular automata operate on a two-dimensional honeycomb lattice where the sites are either populated (A) or vacant (\emptyset , Fig. 1a). They can change their state by local death and birth events. In both models, deaths are Poisson processes:

- $A \rightarrow \emptyset$: A populated site becomes vacant with rate 1.

In our first model, the rate, with which a vacant site becomes populated by a local birth event, is exactly proportional to the number of neighbors:

- $A \rightarrow 2A$: A vacant site at position (x, y) with k populated adjacent sites becomes itself populated at the rate $b(x) \cdot k/6$.

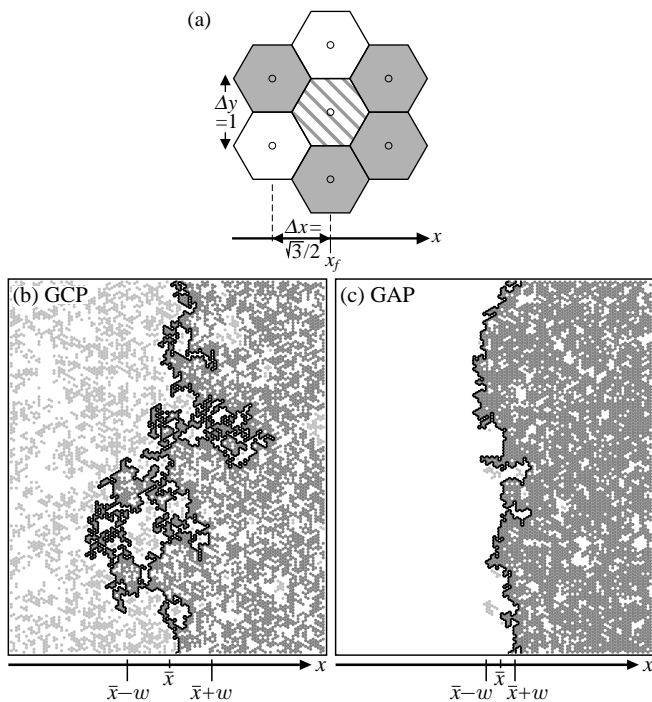


FIG. 1: (a) Sites in the spatial models are placed in the centers of the hexagons in a honeycomb lattice. Gray cells represent populated (A), white cells vacant (\emptyset) sites. In this example, the focal site in the center has $k = 4$ populated neighbors. If this site is populated, it will die during a small time interval dt with probability equal to dt . If, on the other hand, this site is vacant, it will become populated with probability $(k/6)b(x_f)dt$ in the GCP or $[\frac{1}{2}k(k-1)/15]b(x_f)dt$ in the GAP, where $b(x_f)$ is the local birth attempt rate. (b) Typical snapshot of the GCP, (c) of the GAP. Dark gray: the largest populated cluster. Light gray: all other populated sites. Black curve: percolation hull. The mean hull position \bar{x} and the width of the fluctuations w are indicated at the bottom.

The second model implements a local Allee effect by requiring at least one pair of neighbors for successful births. The rule $A \rightarrow 2A$ is replaced with:

- $2A \rightarrow 3A$: A vacant site at (x, y) with k neighbors [i.e., $\frac{1}{2}k(k-1)$ pairs of neighbors] becomes populated with rate $b(x) \cdot \frac{1}{2}k(k-1)/15$.

The denominators 6 and 15 are the maximum number of neighbors and the maximum number of neighbor pairs, respectively. Sites are updated in a random order with the rates stated above following the algorithm of Ref. 10.

The function $b(x)$ can be interpreted as the rate with which an individual in column x attempts to produce offspring on an adjacent site. A birth attempt succeeds only if that site is vacant. In the case of $2A \rightarrow 3A$, success further depends on a second neighbor adjacent to the newly born individual. If $b(x)$ is a constant, then the first model is equivalent to a contact process [11], and our second model becomes a special case of ‘‘Schlogl’s second model’’ [12].

Our work differs from previous studies by assuming a constant gradient $g > 0$ in the birth attempt rate, $b(x) = gx$. Long-range gradients are important in ecology because the environmental conditions can change gradually over distances larger than the distance of dispersal within one generation (e.g., along a hillside or across geographic latitudes). We call $A \rightarrow 2A$ a gradient contact process (GCP) [10, 13] and $2A \rightarrow 3A$ a gradient Allee process (GAP). As long as the initial population density is sufficiently high in regions with high birth rates, the population density reaches a steady state independent of the initial conditions (see supplement).

Because $g > 0$, the steady-state density of populated sites grows in both the GCP and the GAP as x , and hence b , increases. At small x , the populated sites form small isolated patches (light gray sites in Figs. 1b and 1c) whereas at large x most populated sites belong to one large cluster (dark gray). The curve along which the largest cluster touches the largest contiguous vacant area (black curve) is the percolation hull [8, 14]. If the populated sites provide habitat or food for another species, the hull marks the borderline between the connected and fragmented occurrence of this resource. An example is a treeline across an altitudinal or latitudinal gradient. Births and deaths cause the position and shape of the percolation hull to fluctuate. The average position of the hull \bar{x} and the characteristic width of the fluctuations w depend on g and the model (GCP versus GAP). We compute \bar{x} and w as the mean and the standard deviation of the distribution of x -coordinates along the hull during several independent runs.

In Fig. 1(b), the number of sites in the GCP’s largest cluster increases gradually from left to right. The increase is much more abrupt in the GAP (Fig. 1c) which generates fewer isolated clusters. This impression can be confirmed by looking at local densities in the transition region near \bar{x} . Because w is the relevant length scale in this region, we investigate subsystems located between $\bar{x} - w$ and $\bar{x} + w$ (Fig. 2a). We determine the cluster that has the largest number of sites N within a $2w \times 2w$ square. In both models, the mean of N scales approximately as w^{D_f} with $D_f = 91/48$, the fractal dimension of the incipient infinite cluster in standard (i.e., uncorrelated, gradient-free, nondirected) two-dimensional percolation [15] (see supplement). But the distribution of the N sites is different in the two models.

To see this quantitatively, let us define the cluster density ρ as N divided by the number of all (populated or vacant) sites in the square. The distributions of ρ , aggregated over independent runs of the GCP and the GAP, at different y -coordinates and at different times, are shown in Fig. 2b. The GCP distribution has a single peak at intermediate densities whereas the GAP has two local maxima, one at zero and another one at high density. In analogy to thermodynamics, where a bimodal probability distribution of an order parameter is an indication of a

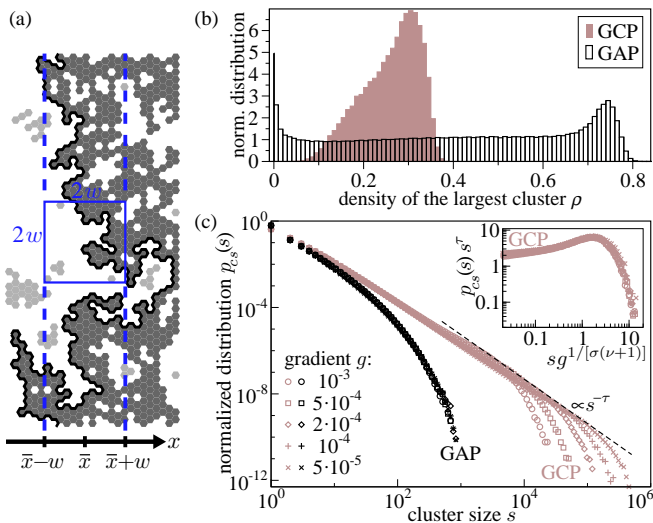


FIG. 2: (a) To distinguish between a continuous and a first-order transition, we investigate squares of dimension $2w \times 2w$ centered at \bar{x} . We measure the fraction of sites ρ that belong to the cluster covering the largest area within the square. (Typically, though not necessarily, this is the largest cluster on the entire lattice, shown in dark gray). (b) From data of several independent runs, we obtain the probability distribution for ρ , represented as a histogram. We show data for $g = 5 \cdot 10^{-5}$. The smaller the gradient, the more weight is concentrated in the two peaks of the GAP distribution. (c) The distribution of cluster sizes s in the stripe $|x - \bar{x}| < w$. We include clusters which are at least partially in this stripe, but exclude the system's largest cluster. The dashed line $\propto s^{-\tau}$ is the tangent to the GCP distribution. The inset shows the data collapse for the GCP. The exponents are those of standard 2D-percolation: $\tau = \frac{187}{91}$, $\sigma = \frac{36}{91}$, $\nu = \frac{4}{3}$ [15].

first-order phase transition [16], percolation in the GAP can be interpreted as a first-order transition between two steady states of either zero or of a positive density. Thus only a population larger than a critical density is able to grow and, when this density is exceeded, the cluster size grows abruptly, reminiscent of recent reports of “explosive percolation” [17], but generated here by a purely local rule.

In some explosive percolation models, cluster sizes were recently shown to follow power-law distributions, casting doubts on whether the transition is truly first order [18]. In the GAP, by contrast, the cluster size distribution $p_{cs}(s)$ in the stripe $|x - \bar{x}| < w$ gives further evidence in support of a first-order transition (Fig. 2c). While the GCP distribution follows the scaling behavior expected for two-dimensional percolation with a continuous transition $p_{cs}(s) = s^{-\tau} f_{cs}(sg^{1/[\sigma(\nu+1)]})$, the GAP distribution does not show indications of scaling. There is neither a power-law decay nor a dependence on the gradient even for large cluster sizes. Instead, consistent with a first-order transition, there is a characteristic size for the GAP clusters.

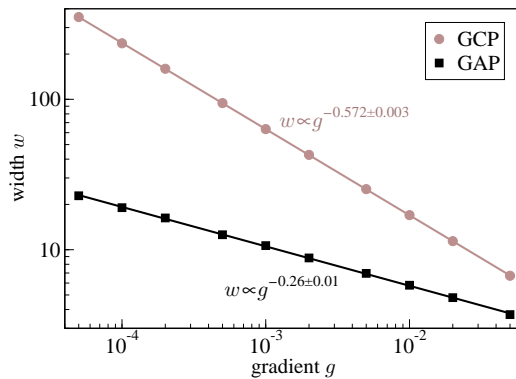


FIG. 3: The hull width w as a function of the gradient g . The lines are least-squares fits to the data. Error bars are smaller than the symbol sizes.

Another percolation property affected by the Allee effect is the scaling relation between w and g (Fig. 3). For the GCP, we find $w \propto g^{-a_{\text{GCP}}}$, $a_{\text{GCP}} = 0.572(3)$ (95% confidence interval). The GAP width also follows a power law, but with a smaller exponent $a_{\text{GAP}} = 0.26(1)$. (The same exponents are observed if the hull is replaced with the accessible external perimeter [19], see supplement.) The exponent a_{GCP} is in agreement with $\nu/(\nu+1) = 4/7$, which was derived for uncorrelated percolation based on the divergence of the correlation length [8]. There is no analogous relation for a_{GAP} , because the correlation length is finite at a first-order transition. The result that w , nevertheless, scales with g in the GAP is surprising, considering that scaling in stochastic gradient models has so far always been linked to divergent correlation lengths [9].

Although the spatial width of the hull increases with decreasing g , the transition zone becomes, in terms of the birth rate b , more confined. This becomes clear by plotting $p_{lc}(b)$, the probability that a site with birth rate b belongs to the largest cluster (Fig. 4). In both models, $p_{lc}(b)$ approaches a limiting function as $g \rightarrow 0^+$ with a sharp increase at the percolation thresholds $b_{p,\text{GCP}} = 2.260(1)$ and $b_{p,\text{GAP}} = 7.7340(3)$. For finite g , $p_{lc}(b)$ obeys the finite-size scaling $p_{lc}(b, g) = g^c f_{lc}(|b - b_p|g^{a-1})$, where a is the hull width exponent (a_{GCP} or a_{GAP}) and f_{lc} is a model-dependent scaling function. In the GCP, we expect $c = \beta/(\nu+1) = 5/84$. For the GAP, however, the first-order transition demands that p_{lc} has a discontinuity in the limit $g \rightarrow 0^+$ and therefore $c_{\text{GAP}} = 0$. The insets of Fig. 4 show a remarkable data collapse for the anticipated exponents.

Why is percolation in the GAP unconventional? Let us denote by $n(b, t)$ the probability that a site with birth attempt rate b is populated at time t . The mean-field equations for n to lowest order in g are

$$\text{GCP: } \frac{\partial n}{\partial t} = -n + b(1-n)n + \frac{g^2}{4}b(1-n)\frac{\partial^2 n}{\partial b^2}, \quad (3)$$

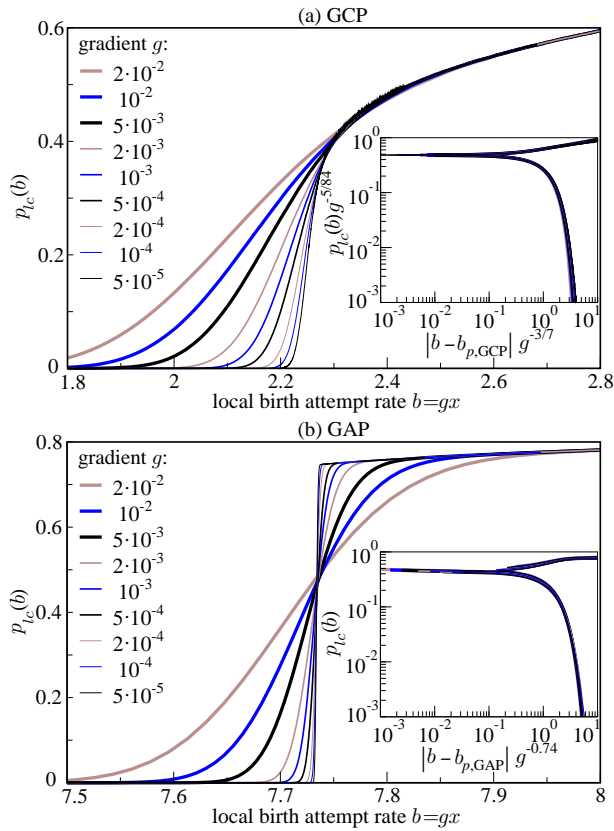


FIG. 4: The probability p_{lc} that a site belongs to the largest cluster as a function of the site's birth attempt rate b in (a) the GCP, (b) the GAP for various gradients g . Insets: The functions collapse if the coordinates are rescaled. In both insets, the same nine data sets are shown as in the main panels.

$$\text{GAP: } \frac{\partial n}{\partial t} = -n + b(1-n)n^2 + \frac{g^2}{10}b(1-n) \left[5n \frac{\partial^2 n}{\partial b^2} - \left(\frac{\partial n}{\partial b} \right)^2 \right], \quad (4)$$

where $b(x) = gx$ (see supplement for the derivation and numerical solutions). If $g = 0$, Eq. 3 turns into the logistic equation (1) with $r = b - 1$, $P = bKn/r$, and Eq. 4 becomes Eq. 2 with $P = n$, $A = 1$, $B = C = b$. For $g \rightarrow 0^+$, Eq. 3 has a continuous stationary solution: $n = \max(0, 1 - 1/b)$. In Eq. 4, on the other hand, n develops a discontinuity in the limit $g \rightarrow 0^+$ where it suddenly jumps from zero to $n \approx 0.77$. If the percolation threshold is at a probability $n_p = 0.5$, as in uncorrelated honeycomb lattices [15], the GCP hull is at a position where $n(b)$ varies smoothly. The GAP hull, by contrast, lies at a position where $n(b)$ changes abruptly.

In summary, the GCP and the GAP behave fundamentally differently near the margin of the populated range. The GCP, a model without any Allee effect, possesses the same characteristic features as previously reported for uncorrelated gradient percolation [10]. The Allee ef-

fect in the GAP changes the situation drastically: the percolation transition is first order and the hull width diverges more slowly for $g \rightarrow 0^+$.

We thank H. J. Jensen, G. Pruessner, O. Peters, R. Dickman, A. O. Parry, A. Windus, G. Csányi and S. Mughal for helpful discussions. M. T. G. gratefully acknowledges support by the German Volkswagen Foundation and Imperial College. B. O. is supported by the Hungarian National Science Foundation (Grant No. OTKA K61534) and the Santa Fe Institute International Program. Calculations were performed on the GOLEM I cluster of the Universität Oldenburg.

-
- [1] W. C. Allee, *Animal Aggregations. A study in General Sociology* (University of Chicago Press, Chicago, 1931).
 - [2] R. W. Brooker *et al.*, *J. Ecol.* **96**, 18 (2008).
 - [3] V. Volterra, *Hum. Biol.* **10**, 1 (1938).
 - [4] R. D. Holt *et al.*, *Oikos* **108**, 18 (2005); M. Roy, K. Harding, R. D. Holt, *J. Theor. Biol.* **255**, 152 (2008).
 - [5] D. M. Johnson *et al.*, *Nature* **444**, 361 (2006).
 - [6] F. Courchamp, L. Berec, and J. Gascoigne, *Allee effects in ecology and conservation* (Oxford University Press, Oxford, 2008).
 - [7] M. A. Lewis and P. Kareiva, *Theor. Popul. Biol.* **43**, 141 (1993); T. H. Keitt, M. A. Lewis, and R. D. Holt, *Am. Nat.* **157**, 203 (2001); T. J. Newman, E. B. Kolomeisky, and J. Antonovics, *Phys. Rev. Lett.* **92**, 228103 (2004); M. G. Clerc, D. Escaff, and V. M. Kenkre, *Phys. Rev. E* **72**, 056217 (2005).
 - [8] B. Sapoval, M. Rosso, and J. F. Gouyet, *J. Physique Lett.* **46**, L149 (1985).
 - [9] A. Hansen *et al.*, *J. Phys. A* **23**, L145 (1990); N. Boissin and H. J. Herrmann, *J. Phys. A* **24**, L43 (1991); S. Roux and E. Guyon, *J. Phys. A* **24**, 1611 (1991); E. S. Loscar, N. Guisoni, and E. V. Albano, *Phys. Rev. E* **80**, 051123 (2009).
 - [10] M. T. Gastner *et al.*, *Am. Nat.* **174**, E23 (2009).
 - [11] T. E. Harris, *Ann. Probab.* **2**, 969 (1974).
 - [12] F. Schlögl, *Z. Phys.* **253**, 147 (1972); P. Grassberger, *Z. Phys. B* **47**, 365 (1982); S. Prakash and G. Nicolis, *J. Stat. Phys.* **86**, 1289 (1997); R. Durrett, *SIAM Review* **41**, 677 (1999); D.-J. Liu, X. Guo, and J. W. Evans, *Phys. Rev. Lett.* **98**, 050601 (2007).
 - [13] B. Oborny *et al.*, *Oikos* **118**, 1453 (2009).
 - [14] R. F. Voss, *J. Phys. A* **17**, L373 (1984).
 - [15] D. Stauffer and A. Aharony, *Introduction to percolation theory* (Taylor & Francis, London, 1991), 2nd ed.
 - [16] J. Lee and J. M. Kosterlitz, *Phys. Rev. Lett.* **65**, 137 (1990).
 - [17] D. Achlioptas, R. M. D'Souza, and J. Spencer, *Science* **323**, 1453 (2009); N. A. M. Araújo and H. J. Herrmann, *Phys. Rev. Lett.* **105**, 035701 (2010); A. A. Moreira *et al.*, *Phys. Rev. E* **81**, 040101(R) (2010).
 - [18] F. Radicchi and S. Fortunato, *Phys. Rev. E* **81**, 036110 (2010); R. M. Ziff, *Phys. Rev. E* **82**, 051105 (2010); R. A. da Costa *et al.*, *Phys. Rev. Lett.* **105**, 255701 (2010).
 - [19] T. Grossman and A. Aharony, *J. Phys. A* **20**, L1193 (1987).